International Journal of Recent Technology and Engineering (IJRTE)
ISSN: 2277-3878, Volume-8 Issue-3, September 2019

Experimental Testing and Numerical Simulations for Typical Swelling Soil in Egypt

Ashraf El-Shamy, Yasser El-Mossallamy, Khalid Abdel-Rahman, Hossam Eldin Ali

Abstract: ***swelling soils exist in many developing urban regions in egypt. Most of these urban regions have new huge developments under constructions. The structures constructed on these swelling soils may be exposed to high damage if any significant change in the moisture content of these swelling soils occures, so the presence of such swelling soils represents a significant hazard. Investigation the behaviour of these swelling soils as well as determination of their swelling parameters has become highly necessary. In this paper, intensive experimental testing program has been conducted on some soil samples collected from some of these regions to determine their swelling parameters. Through this experimental testing program, oedometer swell test has been firstly conducted on same soil with two different techniques; namely different pressure method and huder-amberg method. The procedures and obtained results of the two used methods are discussed and compared showing advantages and shortages of each method. After that, all subsequent experimental tests were perfomred using huder-amberg method as it demonstrated high superiority in determining swelling parameters. Grob's 1d swelling law was applied to all obtained experimental results to give exact and complete determination for all swelling parameters. Furthermore, swelling soil has been simulated numerically via the new user-defined swelling constitutive model which has been recently implemented for the finite element software plaxis. The suitability of this model to simulate the performance of swelling soil is verified by conducting a numerical simulation to one of the huder-amberg oedometer tests through the oedometer soil test facility available in plaxis software. Finally, based on the above-selected experimental approach, swelling parameters were determined from the experimental tests conducted on different soil samples collected from some selected arid/semi-arid regions in egypt. Such test results were summarized and presented as a useful key-parameters of these swelling soils which can be used as pre-determined inputs in any further numerical analyses.***

Keywords: ***Swelling Soil, Oedometer Test, Huder-Amberg Method, Grob's 1D swelling law, Swelling Constitutive Model, Numerical Simulation, Swelling Parameters.***

Manuscript published on 30 September 2019
* Correspondence Author
Ashraf El-Shamy*, Department of Civil Engineering, Ain Shams University, Cairo, Egypt. E-mail: Ashraf.El-Shamy@eng.asu.edu.eg
Yasser El-Mossallamy, Department of Civil Engineering, Ain Shams University, Cairo, Egypt, E-mail: yasser_elmossallamy@eng.asu.edu.eg
Khalid Abdel-Rahman, Department for Underground Construction, Institute for Geotechnical Engineering, Leibniz University, Hannover, Germany, E-mail: khalid@igth.uni-hannover.de
Hossam Eldin Ali, Department of Civil Engineering, Ain Shams University, Cairo, Egypt, E-mail: hossam_e_ali@eng.asu.edu.eg

I. INTRODUCTION

Swelling soils are found at different depths in many arid or semi-arid regions in Egypt where huge developments are under constructions such as El-Mokattam City, El-Qattamiya City, El-Sherouq City, 6 October City, El-Obour City, New Administrative Capital City, New El Alamein City, New Cairo City, Ain El Sokhna and some urban regions in Cairo like Heliopolis. If these swelling soils are exposed to significant change in their moisture content, either due to seasonal variations or any locally changes in the site, more damage will happen to structures. Hence, swelling behaviour investigation and swelling parameters determination for the swelling soils existed in these regions has become extremely important at the present time. In this study, some of these mentioned regions have been selected for performing intensive experimental tests on their swelling soils to determine their swelling parameters. Different soil samples have been collected from swelling soil layers found at different depths at the selected regions. Experimental work has been performed in geotechnical laboratory at faculty of engineering at Ain Shams University.

Oedometer test has been regarded as one of the most important swelling tests that can determine all swelling soil characteristics [1]. Different Oedometer test methods are available in the literature. In all these methods, a soil sample is confined laterally in a rigid mould "Oedometer cell" then subjected to different vertical stresses according to the type of each method [2]. In this study, two different Oedometer test methods; namely Different Pressure method [2], [3] and Huder-Amberg method [4]; were considered. Their procedures and their obtained results are presented, examined and compared.

Grob [5] used the results of Huder-Amberg Oedometer tests [4] and formulated the 1D swelling law between the axial stress σ_i and the final obtained swelling strain $\varepsilon_i^{q(t=\infty)}$ in the same direction as shown in (1).

$$\varepsilon_i^{q(t=\infty)} = \begin{cases} -k_{qi} \cdot log\left(\frac{\sigma_c}{\sigma_{q0i}}\right) & , \sigma_i \geq \sigma_c \\ -k_{qi} \cdot log\left(\frac{\sigma_i}{\sigma_{q0i}}\right) & , \sigma_{q0i} \leq \sigma_i \leq \sigma_c \\ 0 & , \sigma_i \leq \sigma_{q0i} \end{cases} \quad (1)$$

Where: $\varepsilon_i^{q(t=\infty)}$ is the final swelling strain at determined axial stress, k_{qi} is the axial swelling potential, σ_i is the axial stress in the direction of swelling and σ_{q0i} is the maximum swelling stress in that direction. As shown in (1) and Fig. 1, the swelling strains are limited at compressive strength ($\sigma_c = -10$ kPa) to avoid any excessive values at very low compressive stresses or even tensile stresses.

The 3D extension of swelling law was developed by Rissler and Wittke [6]. 3D extension of Rissler and Wittke [6] was proposed by Kiehl [7] based on the results of swelling tests by Pregl et al. [8]. These swelling tests displayed that the principal swelling strains depend only on the principal stresses in those directions.

This was assumed for an isotropic swelling behaviour only. Later, Wittke-Gattermann [9] proposed an approach to extend the 3D swelling law proposed by Kiehl [7] for anisotropic behaviour. Different implementation of Wittke-Gattermann's model [9] was carried out by Heidkamp and Katz [10] and later on by Benz [11].

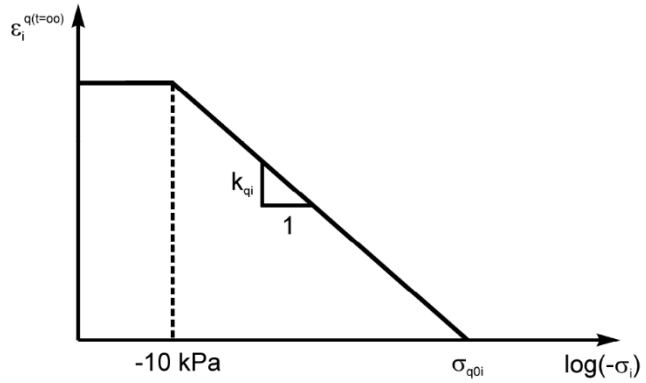

Fig. 1: Grob's semi-logarithmic swelling law (Grob, 1972).

This latest implementation by Benz [11] has been introduced for the finite element software PLAXIS as a new user-defined swelling constitutive model. This new model considers the dependency of swelling strains on stress and time for both swelling clays and rocks. A brief clarification for the model's main features can is given by El-Shamy, El-Mossallamy, Abdel-Rahman and Ali [12]. The fully detailed explanation regarding all constitutive model parameters are found in PLAXIS UDSM-Swelling Rock model [13]. The suitability of this model to simulate the performance of swelling soil is verified by conducting a numerical simulation to one of the Huder-Amberg Oedometer tests through the Soil Test Facility option in PLAXIS software.

II. OEDOMETER SWELL TEST METHODS

A core clay sample was extracted at depth of 21.0 m from executed borehole in "New Administrative Capital City" region located east of Cairo City. The sample was divided, trimmed and prepared in several identical samples for the conducted Oedometer tests. Fig. 2 depicts on the upper the photos of several samples after preparation and placement inside Oedometer rings. Oedometer apparatus at geotechnical laboratory are shown in lower photo of Fig. 2.

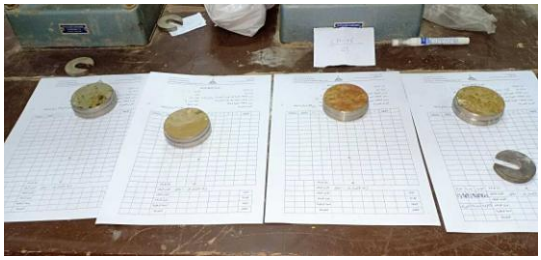

Fig. 2: Swelling clay samples prepared in Oedometer rings and tested in Oedometer apparatus at geotechnical laboratory.

As indicated above, two Oedometer swell test methods were utilized herein. Brief descriptions of the testing preparation, execution methodology and results are presented as follows:

A. *Different Pressure Method*

The statement and procedures of the Different Pressure method is explained as following;

i. Three soil samples (denoted as A, B and C) from the same core sample extracted from depth of 21.0 m were prepared for testing in three oedometer rings. The sample is 63.5 mm diameter and 19 mm thick, enclosed in a circular metal ring and sandwiched between porous stones.

ii. Each sample was loaded at dry state until reaching the stress at which the water should be added. During this stage, each load step is remained for 15 min while monitoring the dial gage readings.

iii. Water was added to the three samples at pre-determined stresses as following;

- First sample (A): At stress equivalent to effective overburden pressure (σ_0') $(\approx 400\ kPa)$
- Second sample (B): At stress equivalent to effective overburden pressure plus expected applied design stress from the building $(\sigma_0' + \Delta\sigma)$ $(\approx 600\ kPa)$
- Third sample (C): At stress equivalent to effective overburden pressure plus twice the expected applied design stress from the building $(\sigma_0' + 2\Delta\sigma)$ $(\approx 800\ kPa$

iv. Each inundated sample was kept loaded with the same stress for at least seven days to observe the expected swelling behavior. Throughout this period, all dial readings were being recorded.

v. After the seven-days inundation period, the samples were further loaded until reaching the maximum available stress $(\approx 1{,}670\ kPa)$ in the testing machine. Each load step was kept for one day (24 hour) while recording the readings.

vi. Finally, the applied loads are removed gradually to full unloading. Each unloading step was followed by one day (24 hour) of heave measurements before another unloading step was administered.

The relationship between applied stress and final obtained total strain for the three samples (A, B and C) are depicted in Fig. 3. Each stress-strain curve is divided into four segments with four different colours to explain the four conducted stages on each sample as following;

i. **Stage 1** represents dry loading until reaching the determined stress at which soaking was implemented.
ii. **Stage 2** represents adding water (inundation) at specific pre-determined stress.
iii. **Stage 3** represents wet loading until reaching the maximum available stress.
iv. **Stage 4** represents gradual unloading until reaching to 10 kPa.

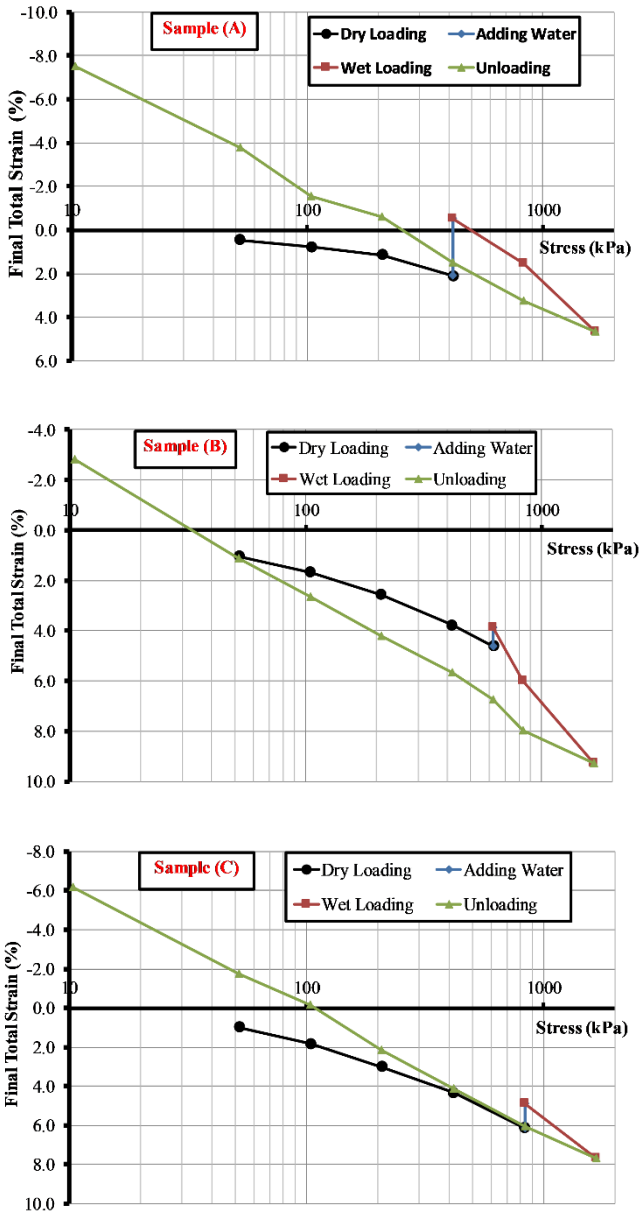

Fig. 3: Stress-Strain results for the three samples (A, B and C) using Oedometer test "Different Pressure Method".

Fig. 4 shows the differential strain (the difference between last total strain value obtained during applying the previous load step and any total strain value resulted at different periods during applying the current load step) observed for each sample at the pre-determined stresses (417, 625 and 834 kPa) during inundation period of 7 days or 10,080 min.

The vertical swelling strain occurred at each pre-determined stress value for each sample is presented in semi-logarithmic curve as shown in Fig. 5. Swelling pressure can be defined as the minimum stress preventing swelling strain. In order to determine it, linear regression trend-line is drawn for the data on logarithmic scale with coefficient of determination or R^2 equal to 0.6087, which represents a rather modest fitting. After that, swelling pressure is calculated using (2) to be 1,210 kPa as presented on Fig. 5. Trying to obtain more accurate results, swelling pressure may be recalculated approximately by neglecting sample (B) and extending the line between samples (A and C) obtaining a parallel line to the linear regression trend-line (same swelling potential) and intersecting with horizontal axis (at zero heave) to be 1,530 kPa as shown in Fig. 5.

$$Y = a\ ln(X) + b\,,$$
$$Vertical\ Swelling\ Strain = a\ ln(Stress) + b$$
$$At\ Swelling\ Pressure\ (x) \rightarrow (Y) = 0$$
$$Swelling\ Pressure\ (x) = EXP(b/a) \qquad (2)$$

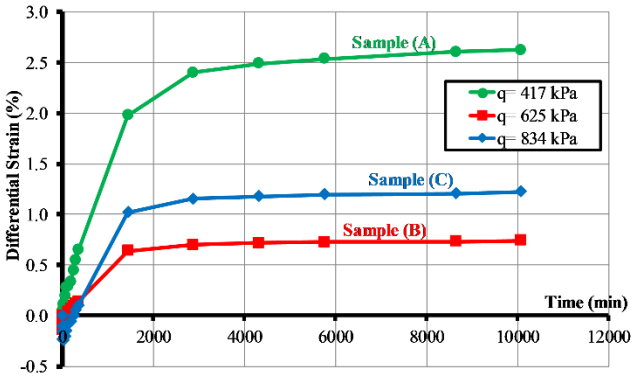

Fig. 4: Time-Differential strain results for the three samples (A, B and C) using Oedometer test "Different Pressure Method".

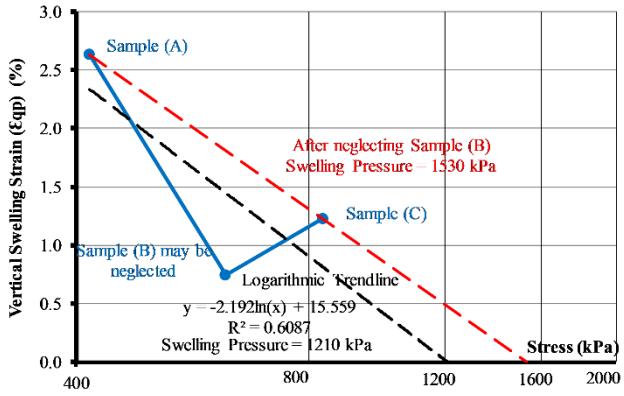

Fig. 5: Swelling pressure determination using Oedometer test "Different Pressure Method".

B. *Huder-Amberg Method*

The statement and procedures of Huder-Amberg method is explained as following;

i. One sample (S00) identical to the previous three samples used in the above-discussed "Different pressure method" at same depth (21m) is prepared. The sample is 63.5 mm diameter and 19 mm thick, enclosed in a circular metal ring and sandwiched between porous stones.
ii. The sample was subjected to loading, unloading and reloading cycle at dry state before adding any water to remove any disturbance happened to the sample in the site. Loading and reloading stages reached to maximum available stress ($\approx 1{,}670\ kPa$). Each loading step in such dry stage was kept for 30 min during the entire loading and reloading stages while only 15 min holding time was allowed during unloading stage.
iii. The water was added to the sample at maximum available stress ($\approx 1{,}670\ kPa$). Readings of dial gage was periodically recorded for 7 days.
iv. The load steps are removed gradually. Through unloading stage after adding water, each load step was maintained for one full day (24 hour) with recording dial gage readings to observe swelling behavior.

Fig. 6 shows the relationship between the applied stress and the corresponding final measured total strain. The curve is divided into four segments with four different colours to explain the four conducted stages as following;

i. **Stage 1** represents dry loading until reaching the maximum available stress.
ii. **Stage 2** represents unloading until reaching to about 100 kPa.
iii. **Stage 3** represents reloading until reaching the maximum available stress.
iv. **Stage 4** represents inundation phase where free water was added to the sample at the maximum available stress followed by unloading until reaching to 10 kPa.

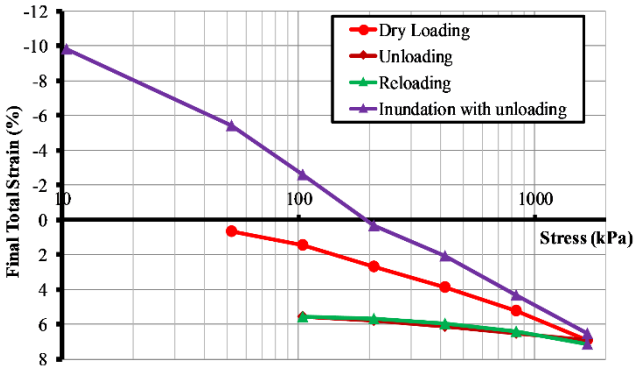

Fig. 6: Stress-Strain results for sample (S00) using Oedometer test "Huder-Amberg Method".

Fig. 7 presents the relationship between time in minutes and differential strain experienced while applying each stress level during Stage 4 presenting inundation and the subsequent unloading phases. The period of maintaining each stress level is as explained before; 7 days for maximum available stress and 1 day for any other stress level. It should be noted that measurements beyond 3,000 min was trimmed in Fig. 7 to attain reasonable scale for x-axis allowing for clear presentation for the results of other stress levels curves. As an exception, the stress level of 52 kPa has been applied for 2 days instead of 1 day due to geotechnical laboratory inaccessibility during the weekend.

The total/cumulative vertical swelling strain occurred at each stress level during Stage 4 "Inundation with unloading" is presented in semi-logarithmic curve as shown in Fig. 8. Logarithmic trend-line is drawn for the data with ($R^2 = 0.9958$) which represents a rather perfect fitting. Accordingly, swelling pressure was estimated, as explained before (2), to be 1,956 kPa. Hence, vertical swelling potential parameter (k_{qp}) can be interpolated from fitting Grob's 1D swelling pattern (1) using the determined swelling pressure (σ_{q0p}) and the maximum swelling strain measured at a minimum limit of stress ($\sigma_c = -10\ kPa$). Theoretical Grob's 1D swelling law is drawn by a dashed red line shown in Fig. 8 and vertical swelling potential parameter (k_{qp}) is calculated to be 7.578 %.

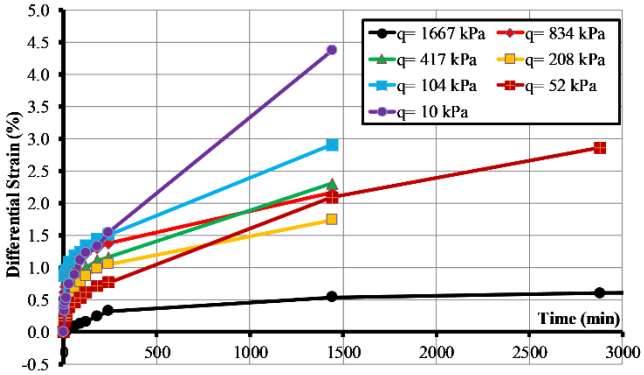

Fig. 7: Time-Differential strain results for sample (S00) at different stress levels using Oedometer test "Huder-Amberg Method".

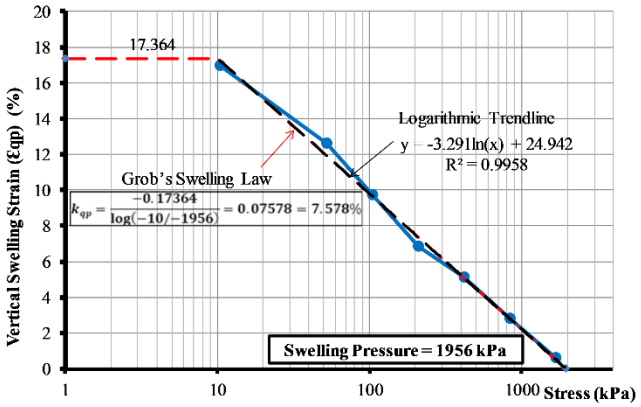

Fig. 8: Swelling parameters calculation using Huder-Amberg Oedometer test method and Grob's 1D swelling law.

C. *Advantages and Uses of Huder-Amberg Method*

The results of the two methods as presented in Fig. 5 and Fig 8, respectively are located on same curve for comparison (see Fig. 9).

The results of "Different Pressure Method" are obtained only at three determined stress levels with low accuracy in calculating swelling pressure and swelling potential compared to "Huder-Amberg Method". This can be attributed to the need for using three samples rather than one sample which are rather dissimilar due inherent natural variability or due to samples preparations. Therefore, the results from Huder-Amberg method would be expected to be more accurate as the testing results are obtained from one sample at different stress levels, which is regarded as a great advantage for Huder-Amberg Oedometer test method compared to any other Oedometer test method. Also, vertical swelling potential parameter (k_{qp}) can be calculated by applying Grob's 1D swelling law to the results as all stress levels are applied during unloading stage from maximum available stress untill minimum limited stress of 10 kPa. Based on the above conclusions, Huder-Amberg method was adopted doing the full subsequent Oedometer tests conducted for experimental analysis for the other collected samples.

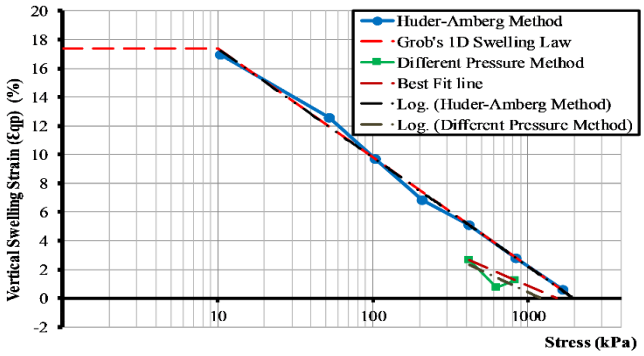

Fig. 9: Comparison between obtained results from "Different Pressure Method" and "Huder-Amberg Method".

As a further advantage, the results obtained from Huder-Amberg method can be used to extend (extrapolate) the "Time-Strain" nonlinear curves to longer periods than the maximum reached time in the laboratory. This can be done by some calculations using the obtained experimental results at each stress level during Stage 4 "Inundation with unloading". This will save the time of maintaining loads to the sample in the laboratory as the curve can be extended to any required time by mathematical calculations using the available laboratory readings.

Firstly, the relation of (Time vs. Time/ Differential Strain) for the laboratory results of each stress level should be calculated and drawn as demonstrated, as an example, in Fig. 10 for two selected stress levels, namely 1,667 kPa and 834 kPa. Using simple linear regression, the best fitting line can be used to determine the differential strain at any time as explained in (3).

$$Y = a\,(X) + b,$$
$$\frac{Time}{Diff.\ Strain(\%)} = a\,(Time) + b,$$
$$Diff.\ Strain(\%) = \frac{Time}{a\,(Time)+b} \quad (3)$$

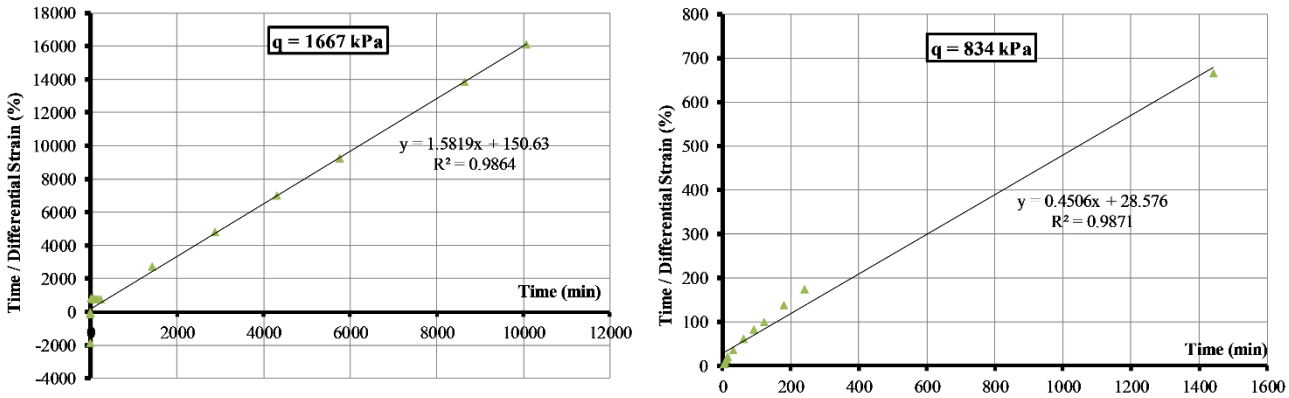

Fig. 10: Relationship between time and (time/ differential strain) for the laboratory results for two stress levels (1,667 and 834 kPa).

For verification purpose, the predicted curve was extended till (7 days or 10,080 min) with (q = 1,667 kPa) which the same time achieved during the test at this stress level. The left chart in Fig. 11, demonstrated significant matching between prediction and tests results. Similarly, for stress (q = 834 kPa), the predicted curve was extended till (3 days or 4,320 min) beyond the testing period that only extended for 1 day or 1,440 min as shown on the right chart in Fig. 11.

Similarly, the relationship between time and cumulative vertical swelling strain $(\boldsymbol{\varepsilon_{qp}})$ is determined at each stress level and drawn to the same above extended periods under the two selected stress levels, namely 1,667 kPa and 834 kPa. Fig. 12 shows relationship between time and total/cumulative vertical swelling strain for both of laboratory results and extrapolated curves for the two selected stress levels.

This will be very helpful for numerical validation as these curves can be compared with the same ones obtained from numerical results as will be presented in **(III)**.

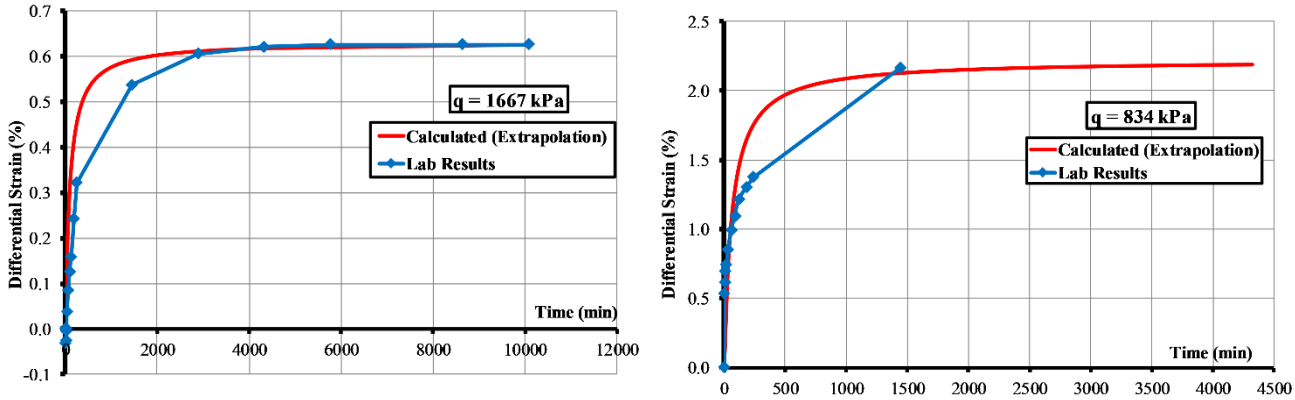

Fig. 11: Time-differential strain results obtained from laboratory and extrapolation calculations for two stress levels (1,667 and 834 kPa).

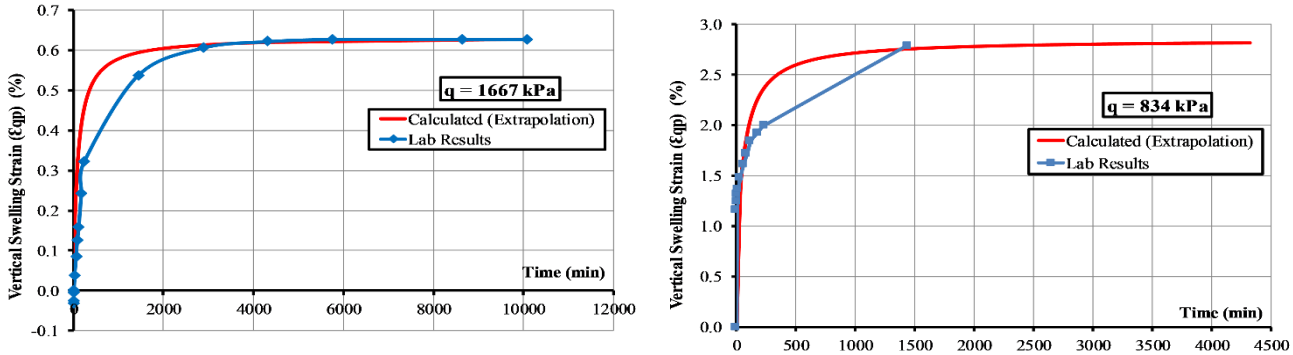

Fig. 12: Time-vertical swelling strain results obtained from laboratory and extrapolation calculations for two stress levels (1,667 and 834 kPa).

III. NUMERICAL SIMULATION OF HUDER-AMBERG OEDOMETER TEST

Through this part, swelling soil has been simulated numerically via the new user-defined swelling constitutive model which has been recently implemented for the finite element software PLAXIS. The suitability of this model to simulate the performance of swelling soil is verified by conducting a numerical simulation to the Huder-Amberg Oedometer test conducted on the same previous clay sample (S00) from "New Administrative Capital City". The obtained numerical results have been verified by comparing with the measured experimental results. This numerical simulation has been conducted through a back-analysis using PLAXIS-VIP,2018 software via Oedometer Soil Test Facility available in it. The loading conditions of Oedometer test simulation are shown in Fig. 13 as an example for an applied vertical stress of -834 kPa which is instantaneously applied in first phase after which in a second phase a swelling time of 3 days is considered in 100 steps.

Fig. 13: Example for loading conditions of Oedometer test.

A. *Determination of Soil Parameters Used in Numerical Simulation*

Using the determined values of swelling pressure $(\sigma_{q0p} = \sigma_{q0t} = 1{,}956\ kPa)$ and vertical swelling potential $(k_{qp} = 7.578\ \%)$ as determined in Fig. 8, a back-analysis for the Oedometer test was conducted for numerical simulation. The routine used as solution procedure for the swelling strain in the model is following Wittke-Gattermann model (Swell_ID = 1). Modulus of elasticity of clay layer $(E_p\ \&\ E_t)$ has been calculated to be approximately 18,200 kPa, which was determined measuring the tangential slope of stress-strain curve of Stage 4 "Inundation with unloading" which represents (E_{un}). Independent shear modulus (G_{pt}) is calculated automatically by PLAXIS using Barden's formula (4).

$$G_{pt} = \frac{E_p}{(1+\frac{E_p}{E_t}+2\nu_{pt})} \quad (4)$$

To remove any contribution of horizontal stresses to the total vertical strains, Poisson's ratio is set to zero, i.e. $(\nu = 0)$ and a very small value of tensile strength (σ_{tens}) (e.g. 0.001 kPa) was needed to be inserted for adjusting the numerical results [14]. Also, horizontal swelling potential parameter is set to zero, i.e. $(k_{qt} = 0)$ as discussed by [12].

Strength parameters are set to be $(c' = 100\,kPa)$ and $(\varphi' = 0°)$ from previous results of direct shear tests conducted on samples from this zone, although, they will not affect on vertical swelling strain results.

All swelling time parameters related to the plasticity (A_{pl}, $\varepsilon_{pl,max}$ and ψ) are set to zero as yield conditions are not reached. Also, A_{el} is set to zero and as a result swelling time parameter η_q is leading to $\left(\eta_q = \frac{1}{A_0}\right)$. The most value for (A_0) which fits with the laboratory results is determined by carrying out the following sensitivity analysis.

B. *Sensitivity Analysis to Determine the Reasonable Swelling Time Parameters*

Sensitivity numerical analysis is conducted considering same periods of the calculated curve that extended from laboratory results for any following comparison between them. Number of steps for each run is set to be constant value of 100. Hence, some Oedometer runs are conducted with two selected stress levels (1,667 and 834 kPa) as an example using some chosen values for A_0 resulting in different values for η_q. Table 1 shows the used values for swelling time parameters and the corresponding maximum obtained vertical swelling strain.

Table 1: Determination of the reasonable value of swelling time parameter (η_q) or (A_0) used in numerical simulation.

A_0 $(1/day)$	η_q (day)	Max numerically obtained vertical swelling strain (ε_{qp}) [%]	
		(q = 1,667 kPa)	(q = 834 kPa)
0.1	10	0.210	0.704
0.5	2	0.455	2.162
1.0	1	0.470	2.648
5	0.2	0.470	2.781
10	0.1	0.470	2.781
50	0.02	0.470	2.781

Fig. 14 depicts upper and lower charts comprising several curves between time and cumulative vertical swelling strain for laboratory tests results, extrapolated calculations based on formulation and numerical simulation results for different values of A_0 or η_q value, for the two selected stress levels of 1,667 and 834 kPa, respectively. From the upper chart in Fig 14, applied for stress level of 1,667 kPa, the maximum obtained vertical swelling strain from numerical simulation results is 0.470% which found to slightly differs from the laboratory tests results (0.626%). This difference is validated through the next analysis **(C)** which is due to applying Grob's 1D swelling law in numerical constitutive model. Furthermore, both charts in Fig. 14 shows that by increasing A_0 value (or decreasing η_q value), swelling rate increases. Also, there is very good agreement between numerical results and those values obtain from laboratory tests provided that a reasonable values range of A_0 or η_q are used. Such suitable range of A_0 value was found to be from 5 to 50 (i.e. from 0.2 to 0.02 for η_q value). In fact, the most matching numerical curve to the test data or simulated data is obtained at $(A_0 = 10)$. Therefore, it was logic to use the same value in all subsequent numerical analyses.

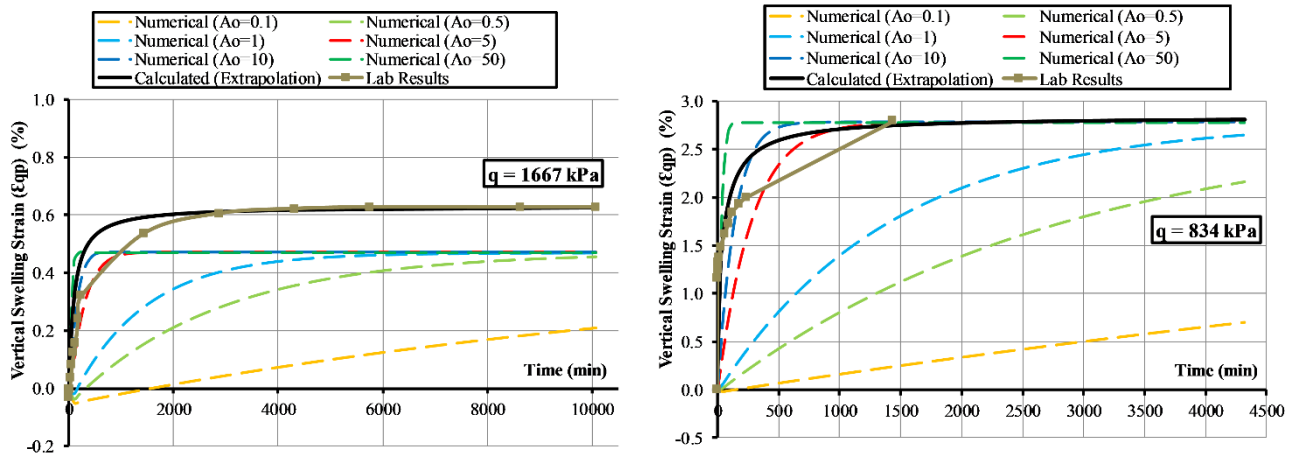

Fig. 14: Numerical verification of swelling strain-time curve through Oedometer test runs for two stress levels (1,667 and 834 kPa).

C. *Numerical Results Verification with Experimental Measurements*

In order to conduct the numerical simulation for the Huder-Amberg Oedometer lab test, different Oedometer test runs are conducted with same laboratory applied stresses with same parameters used in previous study and recommended value for swelling time parameter $(A_0 = 10)$. Table 2 lists the obtained numerical results and the experimental measurements for vertical swelling strain (ε_{qp}) as well as the differences between them. Fig. 15 presents the relationship between applied stress and swelling strain obtained from both the experimental lab results and numerical simulation as well as the Grob's 1D theoretical model. As expected, the obtained numerical simulation results for vertical swelling strain (ε_{qp}) corresponding to all applied stresses are rather identical to the prediction based on Grob's 1D theoretical formulae. This is due to the fact, the new swelling constitutive model in PLAXIS is based on Grob's model.

From the above study, it would be recommended that the swelling characteristics for any swelling soil layer can be determined by conducting Huder-Amberg Oedometer test and then fitting Grob's 1D swelling law to the lab results. These calculated swelling parameters can be used for any further numerical modelling using the newly implemented swelling constitutive model in PLAXIS software.

Table 2: Numerical and experimental results of Huder-Amberg Oedometer test conducted on swelling clay sample.

Applied stress (kPa)	Vertical swelling strain (ε_{qp}) [%]		Differences $\left(\frac{Num.-Exp.}{Exp.}.100\right)$ [%]
	Experimental measurement	Numerical simulation	
10	16.963	17.364	2.4
52	12.595	11.938	-5.2
104	9.732	9.657	-0.8
208	6.826	7.368	7.9
417	5.089	5.074	-0.3
834	2.789	2.781	-0.3
1,667	0.626	0.470	-24.9

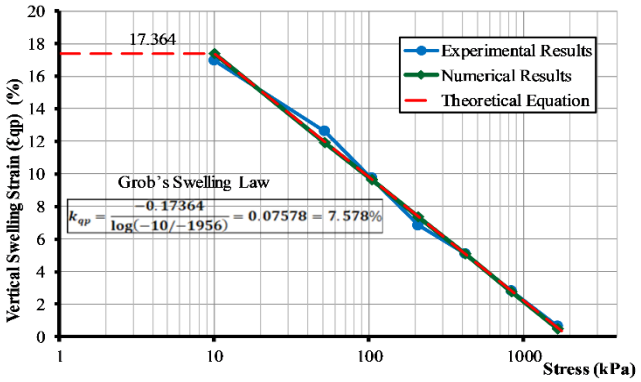

Fig. 15: Numerical results verification with experimental measurements obtained from Huder-Amberg test conducted on the clay sample.

IV. SWELLING SOIL PARAMETERS DETERMINATION FOR SOME ARID REGIONS IN EGYPT

Based on the findings of the pilot study discussed above, wider experimental study was conducted on several soil samples collected from different arid/semi-arid regions in Egypt which currently experience ongoing significant developments and constructions such as; "New Administrative Capital City, New El Alamein City, New Cairo City, Ain El Sokhna and Heliopolis in Cairo". All swelling parameters for the tested swelling soil samples collected from these five selected regions, were determined using the aforementioned recommended approach involving Huder-Amberg Oedometer tests and applying Grob's 1D swelling law to interpolate the test results. The outcome of this testing campaign is summarized and presented in Table 3. This table can be used as a useful key information of the identification of the main swelling characteristics of these soils, which can be used in any further numerical analyses. The calculations of these swelling parameters are clarified with more details in [15].

For example, the swelling layer (encountered at depths ranging from 3 to 5 m) in "New Administrative Capital City" has moderate values of swelling parameters i.e., swelling pressure (from 490 to 825 kPa) and swelling potential (from 1.8 to 8.6 %). This can be clarified by drawing the combination of Grob's 1D swelling law for five core samples collected from this layer from some executed boreholes as shown in Fig. 16. Similarly, Fig. 17 shows the combination of Grob's 1D swelling law for many swelling soil bulk samples in "Ain El Sokhna". These bulk samples were extracted by hand from different sides of excavation site at which construction of some villas is planned. In addition, it was found that these swelling soils has a wide range of swelling parameters i.e., swelling pressure (from 551 to 13,795 kPa) and swelling potential varying from 2.2 to 9.1 %. Furthermore, Fig. 18 shows the combination of Grob's 1D swelling law for four core samples representing swelling layer (encountered at depths ranging from 15 to 20 m) collected from some executed boreholes in "Heliopolis" region in Cairo. It was found that this swelling soil layer has moderate values of swelling parameters i.e., swelling pressure (from 641 to 968 kPa) and swelling potential (from 6.1 to 8.4 %)

It can be concluded from these figures that swelling soil may has high swelling potential but with low swelling pressure and vice versa, In other words, swelling potential do not depend on swelling pressure value. Also, they give suitable range of swelling parameters of these swelling soils which will help in determining their swelling behaviour and can be used as pre-determined inputs in any further numerical analyses.

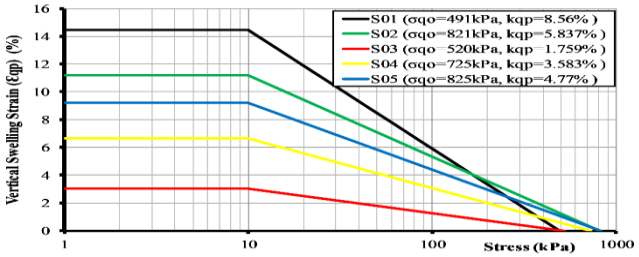

Fig. 16: Combination of Grob's 1D swelling law for samples from the layer (from depth of 3 to 5 m) at "New Administrative Capital City" region.

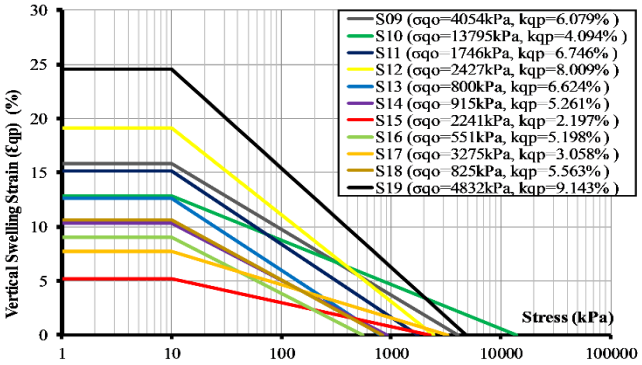

Fig. 17: Combination of Grob's 1D swelling law for samples from swelling soil at "Ain El Sokhna" region.

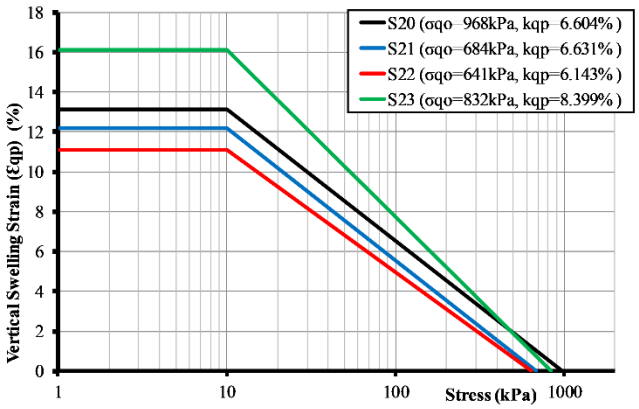

Fig. 18: Combination of Grob's 1D swelling law for samples from the layer (from depth of 15 to 20 m) at "Heliopolis" region in Cairo.

Table 3: Swelling soil parameters determined for different samples collected from some arid regions in Egypt.

Region	Sample ID	Depth (m)	Swelling Pressure (σ_{q0p}) (Kpa)	Vertical Swelling Potential (k_{qp}) (%)
New Administrative Capital City	S00	21	1,956	7.578
	S01	3	491	8.560
	S02	3	821	5.837
	S03	5	520	1.759
	S04	5	725	3.583
	S05	5	825	4.770
New El Alamein City	S06	2	395	1.421
	S07	25	824	7.411
New Cairo City	S08	3 to 4	388	9.414
Ain El Sokhna	S09	NA	4,054	6.079
	S10	NA	13,795	4.094
	S11	NA	1,746	6.746
	S12	NA	2,427	8.009
	S13	NA	800	6.624
	S14	NA	915	5.261
	S15	NA	2,241	2.197
	S16	NA	551	5.198
	S17	NA	3,275	3.058
	S18	NA	825	5.563
	S19	NA	4,832	9.143
Heliopolis, Cairo	S20	15	968	6.604
	S21	17	684	6.631
	S22	18	641	6.143
	S23	20	832	8.399

V. CONCLUSIONS

Based on the experimental testing program conducted for swelling soil samples in Egypt as well as the numerical simulation and validation, the following points can be concluded:

1. The performed tests present and verify a framework of determination of the main characteristics and modeling approaches of swelling soils.
2. Different pressure Oedometer swell test method exhibits some error while getting swelling pressure. It is very expected due to the differences in the testd samples of same soil as they cannot be fully identical. The results from Huder-Amberg method proved to be less erratic as they are obtained from one sample at different stress levels which is regarded an advantage for Huder-Amberg Oedometer test method compared to any other Oedometer test method.
3. Vertical swelling potential parameter (k_{qp}) can be well determined by fitting Grob's 1D swelling law to the experimental results obtained from Huder-Amberg method as all stress levels are applied during unloading stage from maximum available stress until minimum limited compression stress of 10 kPa. More clearly, it would be recommended that the swelling characteristics for any swelling soil layer can be determined by conducting Huder-Amberg Oedometer test and then fitting Grob's 1D swelling law to the experimental results. As another advantage for Huder-Amberg method, "Time-Strain" curves can be extended to longer periods than the maximum reached time in the laboratory via some calculations using the obtained experimental results

at each stress level which will save the time of applying load to the sample in the laboratory.

4. The new user-defined swelling constitutive model implemented recently for PLAXIS software has been validated for numerical simulation of swelling soil by performing a back-analysis to one of the conducted Huder-Amberg Oedometer tests. Furthermore, the best reasonable swelling time parameters have been determined for this selected soil by conducting a sensitivity analysis. Through this analysis, a value of $(A_0 = 10)$ was recommended to use with any numerical analyses of this soil due to its best matching with its obtained experimental results. It can be generally concluded from this sensitivity analysis that swelling rate increases while increasing A_0 value or decreasing η_q value.
5. Useful Key-swelling parameters were determined using the recommended approach for several soil samples collected from five new urban regions in Egypt that experienced significant constructions activities. All determined swelling parameters can be used in any further numerical analyses conducted for these swelling soils.

VI. NOTATIONS

A_0	Initiating time swelling parameter (threshold) [1/day]
A_{el}	Time swelling parameter for elastic volumetric strains [1/day]
A_{pl}	Time swelling parameter for plastic volumetric strains [1/day]
η_q	Time swelling parameter [day]
E_t	Young's modulus parallel to bedding plane $[kN/m^2]$
E_p	Young's modulus normal to bedding plane $[kN/m^2]$
G_{pt}	Independent shear modulus $[kN/m^2]$
k_{qp}	Vertical swelling potential
k_{qt}	Horizontal swelling potential
c'	Effective cohesion $[kN/m^2]$
φ'	Effective friction angle [°]
ψ	Angle of dilatancy [°]
ν_{pt}	Poisson's ratio out of bedding plane
ν_{tt}	Poisson's ratio within bedding plane
$\varepsilon_{pl,max}$	Maximum limit for plastic volumetric strain
ε_{qp}	Vertical swelling strain
σ_c	Minimum compressive strength $[kN/m^2]$
σ_{q0p}	Vertical maximum swelling pressure $[kN/m^2]$
σ_{q0t}	Horizontal maximum swelling pressure $[kN/m^2]$
σ_{tens}	Tensile strength $[kN/m^2]$

REFERENCES

1. M. Barla, "Tunnels in swelling ground-Simulation of 3D stress paths by triaxial laboratory testing," Ph. D. Thesis, Politecnico di Torino, Italy, 1999.
2. ASTM D4546-14, "Standard test methods for one-dimensional swell or collapse of soils," U.S.A, 2014.
3. ECP 202/5, "The foundation on problematic soil," in Egyptian Code of Soil Mechanics and Foundation Design and Construction, Cairo: National Center for Housing and Construction Research, 2001.
4. J. Huder, and G. Amberg, "Quellung in Mergel, Opalinuston und Anhydrit (Swelling in marl, Opalinus and anhydrite)," Versuchsanstalt Fuer Wasserbau Und Erdbau, Eth Zuerich, 1970.
5. H. Grob, "Schwelldruck im Belchentunnel (Swelling pressure in the Belchen tunnel)," in Proc. Int. Symp. für Untertagebau, Luzern, 1972, pp. 99–119.
6. P. Rissler, and W. Wittke, "Bemessung der auskleidung von hohlräumen in quellendem gebirge nach der finite element methode (Dimensioning the lining of cavities in swelling mountain using the finite element method)," Veroffentlichungen des Instituts für Grundbau, Bodenmechanik, Felsmechanik und Verkehrswasserbau der RWTH, vol. 2, pp. 7–46, 1976.
7. J. R. Kiehl, "Ein dreidimensionales Quellgesetz und seine Anwendung auf den Felshohlraumbau (A three-dimensional source law and its application to rock cavity construction)," in Sonderheft der Zeitschrift Geotechnik, Vorträge zum 9. Nationalen Felsmechanik Symposium, 1990.
8. O. Pregl et al., "Dreiaxiale Schwellversuche an Tongesteinen (Three-axial swelling tests on clay stones)," geotechnik, vol. 1, pp. 1–7, 1980.
9. P. Wittke-Gattermann, "Verfahren zur Berechnung von Tunnels in quellfähigem Gebirge und Kalibrierung an einem Versuchsbauwerk (Method for calculating tunnels in swellable rock and calibration at a test facility)," VGE, 1998.
10. H. Heidkamp, and C. Katz, "The swelling phenomenon of soils-Proposal of an efficient continuum modelling approach," in Proc. ISRM Regional Symposium EUROCK, 2004, pp. 743–748.
11. T. Benz, Preliminary documentation of swelling rock model routines for the use of TU Delft only (not publicly published). Norwegian University of Science and Technology (NTNU), 2012.
12. A. El-Shamy, Y. El-Mossallamy, K. Abdel-Rahman, and H. Ali, "Numerical simulation of swelling soil via swelling rock constitutive model," in Fifteenth International Conference on Structural and Geotechnical Engineering, 2018.
13. Plaxis, "Swelling Rock model. User-Defined Soil Model (UDSM), " the Netherlands, 2014.
14. S. Hosseinzadeh, "Numerical assessment and validation of a swelling rock model," M.Sc. Thesis, Delft University of Technology, the Netherlands, 2012.
15. A. El-Shamy, "Performance of swelling soil in arid areas by applying enhanced numerical analysis," Ph. D. Thesis, Ain Shams University, Egypt, unpublished.

AUTHORS PROFILE

Ashraf El-Shamy is a teaching assistant of geotechnical engineering at Ain Shams University, Cairo, Egypt. He is currently doing his Ph.D in geotechnical engineering, civil engineering department. He obtained his B.Sc. degree (2012) and M.Sc. degree (2016) in civil engineering from Ain Shams University. His research interests are in tunneling & underground structures, swelling soil behavior, soil-structure interaction and numerical modelling. He has a wide experience by the design and construction of different shallow and deep foundations as well as various earth-supporting systems through participating in many geotechnical projects in Egypt, Turkey and Saudi Arabia. He has published research articles in peer-reviewed international journals and conferences.

Yasser El-Mossallamy is a chair professor of geotechnical engineering at Ain Shams University, Cairo, Egypt. He has been a researcher and consultant since 32 years. His work includes among others the application of numerical modeling and analyses in geotechnical projects. He has a wide experience by the design and construction of raft and piled raft foundations of high-rise buildings and bridge foundation. He was also involved in many projects dealing with special measures to increase stability of landslides, soil improvement, rock fall hazards and tunneling. He has shared a lot of mega projects in different countries especially in Germany, China, Turkey, Egypt, Saudi Arabia, Kuwait UAE and Jordanian. He has more than 100 publications dealing with different geotechnical topics.

Khalid Abdel-Rahman is working right now as "Deputy Head" at Institute for Geotechnical Engineering - University of Hannover - Germany. He got his PhD degree from University of Dortmund-Germany.

His Special field is the “Design of Foundation Systems for Wind Energy Plants”. He has a wide experience by the design and construction of monopiles and numerical modelling for different geotechnical systems. He was also involved in many projects dealing with design of piles for offshore wind energy foundations in Germany. During his academic career, he published more than 80 publications in Geotechnical field. Last but not least, he won “2015 Outstanding Paper Award” from the international journal “Computers and Geotechnics”.

Hossam Eldin Ali is an associate professor of geotechnical engineering at Ain Shams University, Cairo, Egypt. Through more than 26 years of practical and academic work, he has a wide experience in teaching, design and analysis of different geotechnical systems in several countries including Egypt, Oman, Algeria and Saudi Arabia. His work includes among others the application of numerical modeling and analyses in geotechnical projects. He was also involved in many projects dealing with earth dams, ground improvement, lab and in-situ soil testing and underground excavation. He has published many research articles in peer-reviewed international journals and conferences dealing with different geotechnical topics.